Nuclear Materials and Energy 22 (2020) 100723

Contents lists available at ScienceDirect

Nuclear Materials and Energy

journal homepage: www.elsevier.com/locate/nme

Dose rates and specific activities of copper based materials irradiated during the TT plasma operation at JET

Andrius Tidikas, Simona Breidokaite*, Andrius Slavickas, Gediminas Stankunas, JET Contributors[1]

Lithuanian Energy Institute, Laboratory of Nuclear Installation Safety, Breslaujos st. 3, LT-44403 Kaunas, Lithuania

ARTICLE INFO

Keywords:
JET
Fusion
Neutron irradiation
MCNP5
FISPACT

ABSTRACT

Before deuterium-tritium (DTE2), a new tritium campaign (TT) with the objective to validate the activities, dose rates for selected materials and OLTIS container components, as resulting from neutron irradiation at Joint European Torus (JET), is planned. This paper describes the activation and dose rate calculation performed for copper based materials irradiated throughout the foreseen TT plasma operation. Preparatory experiments and calculations are in progress for TT campaign to measure neutron flux spectrum at the irradiation position using dosimetry foils. In addition, the materials to be considered for irradiation during the TT campaign of the OLTIS were identified and analyzed in this study: Al-Bronze and CuCrZr. The neutron-induced activities and dose rates at shutdown were calculated by activation inventory code FISPACT-2010 using the neutron fluxes and spectra provided by the detailed MCNP5 neutron transport calculations. After the irradiation, the activities and dose rates are calculated at several cooling times after the end of irradiation. Highest dose rates the end of irradiation are attributed to Cu-64 radionuclide. Co-58 and Co-60 are the most dominant radionuclides during intermediate and long cooling periods. Highest activities are ascribed to Cu-64 at the beginning and Ni-63 at the end of investigation time.

1. Introduction

Throughout all stages of nuclear fusion reactor with inclusion of final decommissioning and waste management, it is important to evaluate material quantities related to nuclear safety, i.e. specific activities and radiation dose rates, which are critical for the safe operation of the future fusion reactors such as ITER. Currently, research at JET is focused on ITER development and operation. Acquired knowledge and experience at JET should lead to more straightforward exploitation of ITER facilities [1].

Tritium campaign (TT) is proposed to take place at JET in 2020 before the long awaited DTE2 [2]. High neutron yield from the TT and DT fusion reactions (due to residual D in the plasma), as well as the large irradiation surface available at JET will allow to expand the neutron induced activation detection range achievable with the existing DT neutron sources [3].

Material samples will be irradiated along the TT campaign in the Outer Long Term Irradiation Station (OLTIS) [4], which will be located inside the JET vessel at outboard midplane, where the maximum neutron fluence will be achieved and then retrieved after the end of the TT campaign [3]. The OLTIS box in details is shown in Fig. 1.

In preparation for JET DTE2 experiment and during the 2020 JET TT campaign, material irradiation at the OLTIS box location will be measured using activation foils. Objective of the present work is to calculate activities, contact dose rates and dose rates at 30 cm distance from the point source of copper based alloys (see Table 1 for more details). For the safe ITER operations it is necessary to evaluate high thermal conductivity materials which should be interposed between the armour and the cooling channels. For this reason two types of alloys were selected: CuCrZr, Al-Bronze [5,6].

Sample materials and OLTIS itself, will be later exposed to the neutron fluence produced during the DTE2 at JET. The samples and components will be exposed for the whole duration of the campaign in special holders at the outboard midplane close to the poloidal limiters where the neutron flux is highest. After irradiation, the samples will be retrieved to measure the neutron induced activities in structural materials and the degradation of physical properties in functional materials.

* Corresponding author.
E-mail address: simona.breidokaite@lei.lt (S. Breidokaite).
[1] EUROfusion Consortium, JET, Culham Science Centre, Abingdon, UK. See the author list of “X. Litaudon et al. 2017 Nucl. Fusion 57 102001.

https://doi.org/10.1016/j.nme.2019.100723
Received 25 September 2019; Received in revised form 8 November 2019; Accepted 9 November 2019
Available online 19 December 2019

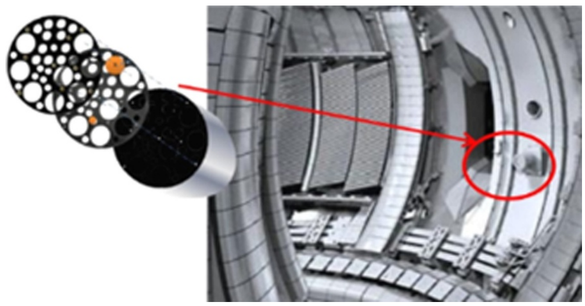

Fig. 1. OLTIS and its position in the vacuum vessel of JET [4].

Table 1
Material composition.

Material	wt% [10^{-2} g/g]	Material	wt% [10^{-2} g/g]
Al-Bronze		CuCrZr	
Cu	81.8365	Cu	99.15
Al	8.73	Cr	0.75
Ni	4.96	Zr	0.1
Fe	4.26		
Mn	0.18		
Zn	0.016		
Si	0.01		
Sn	0.005		
Co	0.0005		
Cd	0.0005		
Nb	0.0005		
Ta	0.0005		
Pb	0.0005		

Dose rate calculation at 30 cm distance from the point source was chosen as it is a convenient distance for possible measurements. It is also a minimum distance allowed in FISPACT code set to prevent float errors. Dose rate calculation in FISPACT is based on deterministic method that involves attenuation equation for air. Energy spectrum histogram for previous equation in form of energy bins is provided by FISPACT activation inventory calculations. MCNP5 is based on stochastic method where individual particle history is simulated and governed by probability distributions. While MCNP5 is also capable of dose rate calculations, it can't account for radionuclide evolution after activation without additional tools.

2. Material composition and irradiaton scenarios

For the calculation of the activation, the following materials are planned to be irradiated during the DTE2 campaign of the OLTIS:

Activation of copper based materials (Al-Bronze and CuCrZr) was investigated. These materials are in consideration for ITER breeder blanket and divertor application where high neutron loads are possible [5].

In CuCrZr composition consists of 3 elements with following percentage: Cu–99%, Cr 0.75% and Zr–0.1% [7]. In Al-bronze one can see 13 different elements, but just 4 of them are more than 1%: Cu–82% Al–8%, Ni–5% and Fe–4% [8]. More information is shown in Table 1.

Neutron flux densities and spectra for OLTIS was provided by the detailed MCNP5 neutron transport calculation code, which has capabilities for simulation of nuclear processes and interactions between wide range of particles including neutrons, photons, electrons and other [9].

Subsequently neutron flux calculation, neutron induced activities and dose rates at shutdown are calculated by means of the code that is capable of performing the modeling of the activation, transmutations and burn up induced by neutron and other particles incident of mater - FISPACT-2010 [10]. Cross section data for neutron induced reactions was taken from EAF-2010. [11].

For the comparison, the neutron flux energy spectra, normalized to one source neutron, are shown in Fig. 2 for DT and TT (DT for comparison reason).

The irradiation scenario used for this analysis assumes a JET operation over 92 days is complex irradiation scenario for TT operation assumes a JET operation during the whole duration of the campaign with the corresponding neutron budget for each of the campaign as shown in Fig. 3 [12].

The MCNP5 model of OLTIS in JET vacuum vessel is shown in Fig. 4. The TT neutron flux spectrum in the Vitamin-J 175 group format for OLTIS was considered in the position at OLTIS-L $R = 400$.

In Vitamin-J 175 group format neutrons are divided in 175 energy groups that cover energy range from 0.1 eV to 19.6 MeV. [10].

The activities and dose rates were calculated at the end of the irradiation and for cooling times of 0 and 1 s, 1 min, 1 h, 1 day, 1 week, 1 month and 1 year after the irradiation.

In the UK any material with an activity below 12 MBq/kg is classified as a low level Radioactive Waste and requires no treatment before final disposal [13].

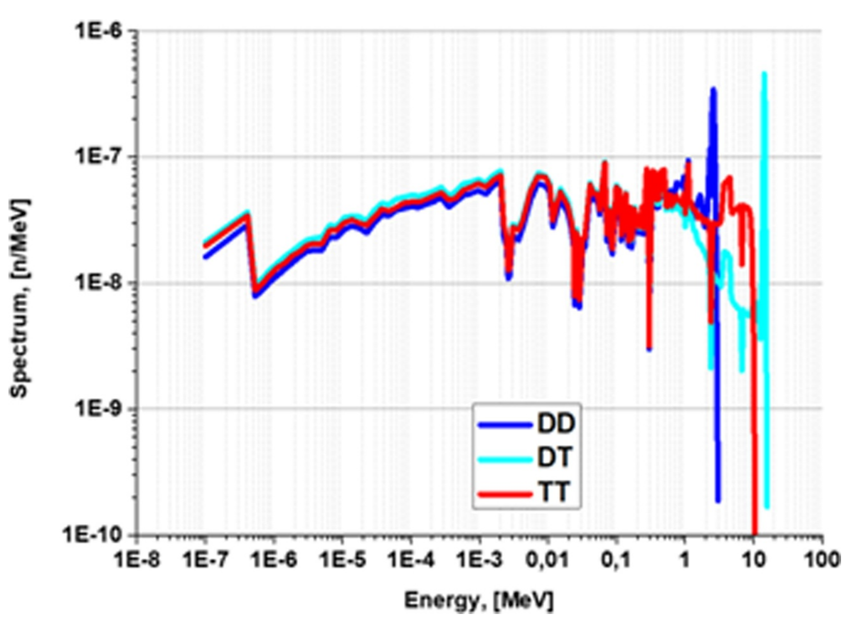

Fig. 2. TT, DT and DD (for comparison) neutron flux spectrum at OLTIS.

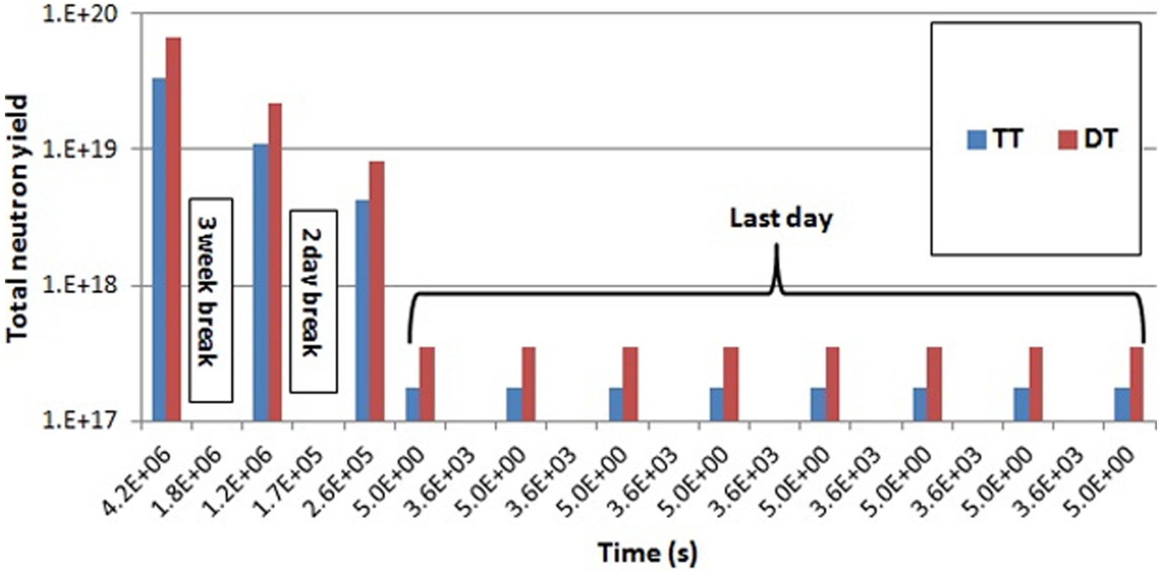

Fig. 3. The irradiation scenario used for this analysis assumes a JET operation.

3. Calculation results

This section contains data of neutron induced activities, contact dose rates and dose rates at 30 cm distance from the point source of 1 g of material, together with the most contributing radionuclides identified. Results were calculated using neutron flux densities and spectra for OLTIS container. Radionuclide analysis for nuclides that contribute more than 1% to the total value to the activation characteristics during investigated time periods is presented.

3.1. AL-Bronze

From the study of the two types of copper based alloys, some tendencies in the dominating radionuclides can be outlined. Firstly, Al-Bronze shortly after the end of the irradiation campaign is dominated by Cu-64 (half-life 12.7 h, β^+, β^-), which is the largest contributor to the activity within the first days after the end of irradiation followed by Cu-66 (half-life 5,1 month, β-) and Co-58 (half-life 70.85 day, β^+). Because of longer half-life after one year of calculation time Ni-63 (half-life 101.1 year, β^-) is the most dominant radionuclide. The value of total specific activity is decreasing from 289.37 MBq/kg–0.685 MBq/kg throughout observation time. (see Fig. 5, Table 2a)

Neutron capture leading to either gamma or proton emission was main reaction in the most important radionuclides. Cu-64 is being produced by (n, g) reaction from Cu-63. Co-58 was produced by (n, p) reaction from Ni-58. And for Ni-63 there are two possible pathways: 3% probability for Ni-62 (n, g) reaction and 97% probability for Cu-63 (n, p) reaction.

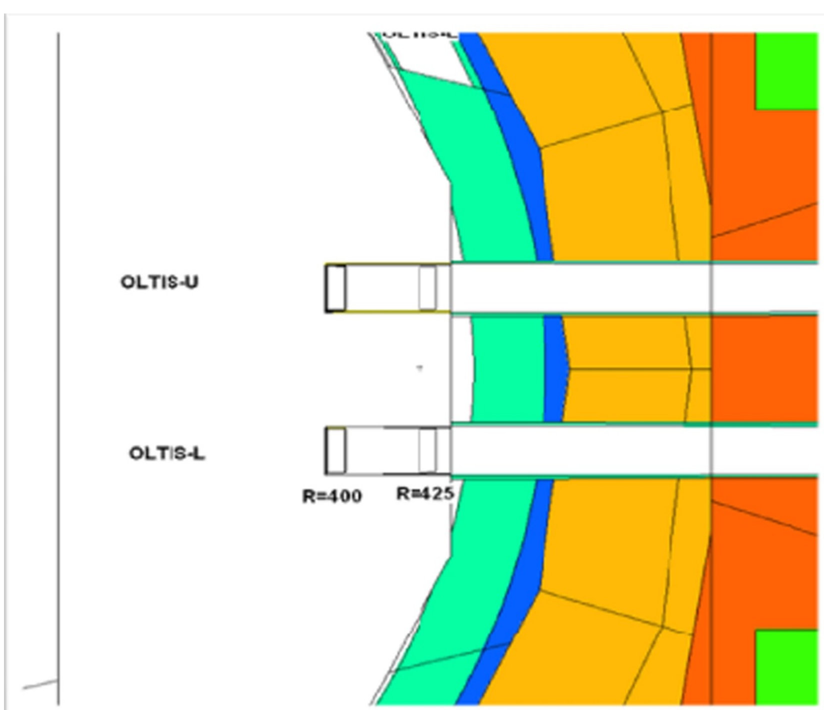

Fig. 4. MCNP model of JET at the location of OLTIS.

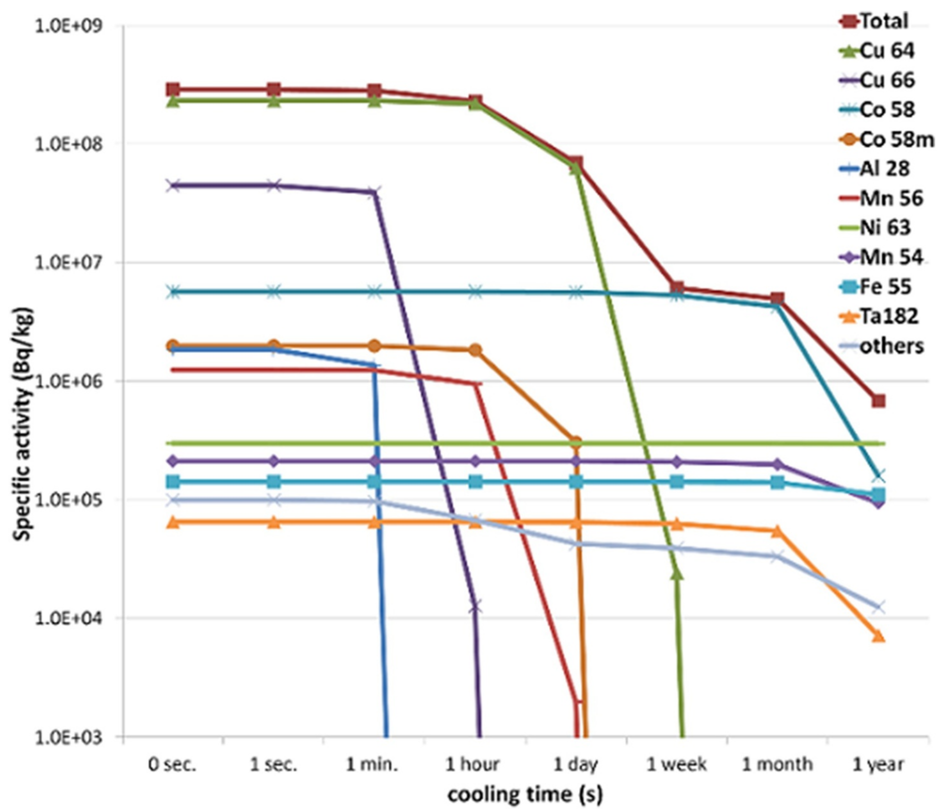

Fig. 5. Specific activity at OLTIS for Al-Bronze.

Similarly, the dose rate at the source surface and at 30 cm distance is mainly influenced by Cu-64 at the end of irradiation time until one week, then it decays and Co-58 starts to dominate. In case of dose rates with distance 30 cm from the surface, dose rate values are approximately 10^4 times smaller compared to corresponding contact dose rates (Figs. 6). The values of total dose rate are decreasing from 13.29 mSv/h to 68.11 μSv/h (see Table 3a), dose rate 30 cm away from source is decreasing from 223.18 nSv/h to 0.69 nSv/h throughout the investigated cooling periods (see Table 4a).

3.2. CuCrZr

The investigated CuCrZr material, which consist of larger copper fraction 99.15% compared to 88.34% of Al-Bronze, shows similar

Table 2
Specific activity Bq/kg at OLTIS a) Al-Bronze, b) CuCrZr.

a)								
Cooling time(s)	0.00E + 00	1.00E + 00	6.00E + 01	3.60E + 03	8.64E + 04	6.05E + 05	2.59E + 06	3.15E + 07
Total	2.8937E + 08	2.8926E + 08	2.8297E + 08	2.2988E + 08	6.9594E + 07	6.1062E + 06	4.9820E + 06	6.8528E + 05
Cu-64	2.33E + 08	2.33E + 08	2.33E + 08	2.21E + 08	6.29E + 07	2.43E + 04	~0	~0
Cu-66	4.48E + 07	4.47E + 07	3.91E + 07	1.29E + 04	~0	~0	~0	~0
Co-58	5.70E + 06	5.70E + 06	5.70E + 06	5.69E + 06	5.65E + 06	5.33E + 06	4.25E + 06	1.61E + 05
Co-58m	1.99E + 06	1.99E + 06	1.98E + 06	1.84E + 06	3.07E + 05	~0	~0	~0
Al-28	1.86E + 06	1.85E + 06	1.36E + 06	~0	~0	~0	~0	~0
Mn-56	1.25E + 06	1.25E + 06	1.24E + 06	9.55E + 05	1.99E + 03	~0	~0	~0
Ni-63	3.01E + 05	3.01E + 05	3.01E + 05	3.01E + 05	3.01E + 05	3.01E + 05	3.01E + 05	2.99E + 05
Mn-54	2.13E + 05	2.13E + 05	2.13E + 05	2.13E + 05	2.13E + 05	2.10E + 05	2.00E + 05	9.49E + 04
Fe-55	1.43E + 05	1.43E + 05	1.43E + 05	1.43E + 05	1.43E + 05	1.42E + 05	1.40E + 05	1.11E + 05
Ta-182	6.56E + 04	6.56E + 04	6.56E + 04	6.56E + 04	6.52E + 04	6.29E + 04	5.47E + 04	7.23E + 03
others	1.00E + 05	1.00E + 05	9.80E + 04	6.76E + 04	4.29E + 04	3.93E + 04	3.33E + 04	1.26E + 04
b)								
Cooling time(s)	0.00E + 00	1.00E + 00	6.00E + 01	3.60E + 03	8.64E + 04	6.05E + 05	2.59E + 06	3.15E + 07
Total	3.3705E + 08	3.3692E + 08	3.2989E + 08	2.6779E + 08	7.6673E + 07	5.0516E + 05	4.2801E + 05	3.5187E + 05
Cu-64	2.82E + 08	2.82E + 08	2.82E + 08	2.67E + 08	7.62E + 07	2.94E + 04	~0	~0
Cu-66	5.43E + 07	5.42E + 07	4.74E + 07	1.56E + 04	~0	~0	~0	~0
Cr-51	1.20E + 05	1.20E + 05	1.20E + 05	1.20E + 05	1.17E + 05	1.01E + 05	5.67E + 04	1.30E + 01
Ni-63	3.53E + 05	3.53E + 05	3.53E + 05	3.53E + 05	3.53E + 05	3.53E + 05	3.53E + 05	3.51E + 05
Nb-97	7.09E + 03	7.09E + 03	7.09E + 03	7.06E + 03	2.83E + 03	~0	~0	~0
Zr-97	7.09E + 03	7.09E + 03	7.08E + 03	6.80E + 03	2.62E + 03	6.76E + 00	~0	~0
Zr-95	1.00E + 04	1.00E + 04	1.00E + 04	1.00E + 04	9.89E + 03	9.27E + 03	7.23E + 03	1.92E + 02
others	2.25E + 04	2.25E + 04	2.20E + 04	1.94E + 04	1.50E + 04	1.22E + 04	1.08E + 04	6.41E + 02

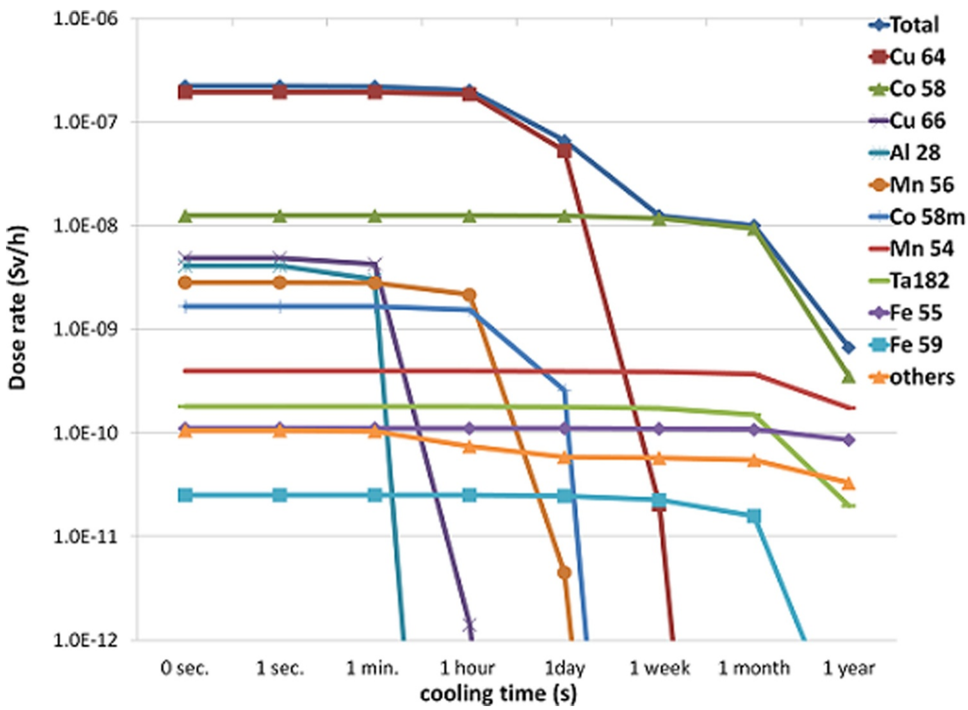

Fig. 6. Dose rate at 30 cm distance from the point source for Al-Bronze.

Table 3
Dose rate Sv/h at OLTIS a) Al-Bronze, b) CuCrZr.

a) Cooling time s	0.00E + 00	1.00E + 00	6.00E + 01	3.60E + 03	8.64E + 04	6.05E + 05	2.59E + 06	3.15E + 07
Total	1.3288E−02	1.3280E−02	1.2869E−02	1.0605E−02	3.9376E−03	1.3954E−03	1.1228E − 03	6.8119Ev05
Cu-64	9.12E−03	9.12E−03	9.11E−03	8.63E-03	2.46E-03	9.51E-07	~0	~0
Al-28	1.06E−03	1.06E−03	7.81E−04	~0	~0	~0	~0	~0
Cu-66	9.83E−04	9.81E−04	8.58E−04	2.83E−07	~0	~0	~0	~0
Co-58	1.41E−03	1.41E−03	1.41E−03	1.41E−03	1.39E−03	1.32E−03	1.05E − 03	3.96E − 05
Mn-56	6.28E-04	6.28E-04	6.25E−04	4.80E−04	1.00E−06	~0	~0	~0
Mn-54	4.67E−05	4.67E−05	4.67E−05	4.67E−05	4.66E−05	4.60E−05	4.37E − 05	2.08E − 05
Ta-182	2.23E−05	2.23E−05	2.23E−05	2.23E−05	2.21E−05	2.13E−05	1.86E − 05	2.45E − 06
Fe-59	5.27E−06	5.27E−06	5.27E−06	5.26E−06	5.19E−06	4.72E−06	3.30E − 06	1.79E − 08
others	1.49E−05	1.49E−05	1.47E−05	1.13E−05	7.55E−06	7.37E−06	7.17E − 06	5.25E − 06

b) Cooling time	0.00E + 00	1.00E + 00	6.00E + 01	3.60E + 03	8.64E + 04	6.05E + 05	2.59E + 06	3.15E + 07
Total	1.2290E−02	1.2287E−02	1.2128E−02	1.0503E−02	2.9968E−03	5.6372E−06	3.6437E − 06	2.7101E − 07
Cu-64	1.11E−02	1.11E−02	1.11E−02	1.05E−02	2.99E−03	1.16E−06	~0	~0
Cu-66	1.20E−03	1.20E−03	1.05E−03	3.45E−07	~0	~0	~0	~0
Zr-95	1.74E−06	1.74E−06	1.74E−06	1.74E−06	1.72E−06	1.61E−06	1.26E − 06	3.35E − 08
Nb-97m	1.16E−06	1.16E−06	1.16E−06	1.12E−06	4.31E−07	~0	~0	~0
Nb-97	1.12E−06	1.12E−06	1.12E−06	1.12E−06	4.48E−07	~0	~0	~0
Nb-95	2.21E−06	2.21E−06	2.21E−06	2.21E−06	2.20E−06	2.15E−06	1.90E − 06	7.56E − 08
Cr-51	6.38E−07	6.38E−07	6.38E−07	6.37E−07	6.22E−07	5.35E−07	3.01E − 07	6.89E − 11
Co-60	1.85E−07	1.85E−07	1.85E−07	1.85E−07	1.84E−07	1.84E−07	1.83E − 07	1.62E − 07
Others	3.83E−07	3.83E−07	3.82E−07	3.49E−07	1.10E−07	1.13E−09	6.73E − 10	2.22E − 11

trends in activity: at the beginning of cooling time, where Cu-64 is the main contributor for first few days followed by Cu-66. At the end of the cooling time, Ni-63 becomes the most dominant radionuclide. The value of total specific activity is decreasing from 337.05 MBq/kg to 0.35 MBq/kg. (see Fig. 7, Table 2b)

Regarding the dose rates radionuclide hierarchy differs: at the beginning of observation time highest dose rate belongs to Cu-64 radionuclide within the first few days after the end of irradiation, but at the end of observation time—Zr-95 (half-life 64.03 days, β^-), Nb-95 (half-life 34.99 days, β^-) and Co-60(half-life 5.274 year, β^-) exhibit the highest dose rates. The total value of dose rate is decreasing from 12.29 mSv/h to 0.27 μSv/h. (see Fig. 8, Table 3b). The total value of dose rate at 30 cm distance from point source is decreasing from 243.81 nSv/h to 1.44 pSv/h throughout observation time. (see Table 4b).

All of these isotopes came after different reactions in comparison to Al-Bronze case except Cu-64. For Ni-63 isotope to appear there is just one possible reaction Cu-63 (n, p). In addition, the same reaction occurs for Cr-51 from Cr-50. Similarly, Co-60 will be produced after Cu-63 (n, α) reaction. Isotope Nb-95 could be observed after two reactions: Zr-94 (n, g) and Zr-95 (b-).

Table 4
Dose rate 30 cm away from point source Sv/h at OLTIS a) Al-Bronze, b) CuCrZr.

a)								
Cooling time	0.00E + 00	1.00E + 00	6.00E + 01	3.60E + 03	8.64E + 04	6.05E + 05	2.59E + 06	3.15E + 07
Total	2.2318E−07	2.2315E−07	2.2126E−07	2.0291E−07	6.6477E−08	1.2543E − 08	1.0098E − 08	6.6915E − 10
Cu-64	1.96E−07	1.96E−07	1.96E−07	1.86E−07	5.30E-08	2.05E − 11	~0	~0
Co-58	1.26E−08	1.26E−08	1.26E−08	1.26E−08	1.25E-08	1.18E − 08	9.40E − 09	3.55E − 10
Cu-66	4.89E−09	4.88E−09	4.27E−09	1.41E−12	~0	~0	~0	~0
Al-28	4.13E−09	4.11E−09	3.03E−09	~0	~0	~0	~0	~0
Mn-56	2.83E−09	2.83E−09	2.82E−09	2.17E−09	4.51E−12	~0	~0	~0
Co-58m	1.67E−09	1.67E−09	1.67E−09	1.55E−09	2.58E−10	~0	~0	~0
Mn-54	3.95E−10	3.95E−10	3.95E−10	3.95E−10	3.94E−10	3.89E − 10	3.69E − 10	1.76E − 10
Ta-182	1.80E−10	1.80E−10	1.80E−10	1.80E−10	1.79E−10	1.73E − 10	1.50E − 10	1.99E − 11
Fe-55	1.11E−10	1.11E-10	1.11E−10	1.11E−10	1.11E−10	1.10E − 10	1.08E − 10	8.59E − 11
Fe-59	2.52E−11	2.52E−11	2.52E−11	2.51E−11	2.48E−11	2.26E − 11	1.58E − 11	8.54E − 14
Others	1.06E−10	1.06E−10	1.04E−10	7.43E−11	5.87E−11	5.75E − 11	5.50E − 11	3.30E − 11
b)								
Cooling time	0.00E + 00	1.00E + 00	6.00E + 01	3.60E + 03	8.64E + 04	6.05E + 05	2.59E + 06	3.15E + 07
Total	2.4381E−07	2.4378E−07	2.4283E−07	2.2525E−07	6.4266E−08	1.0643E − 10	5.2818E − 11	1.4497E − 12
Cu-64	2.38E − 07	2.38E − 07	2.38E − 07	2.25E − 07	6.42E − 08	2.48E − 11	~0	~0
Cu-66	5.93E − 09	5.91E − 09	5.17E − 09	1.70E − 12	~0	~0	~0	~0
Cr-51	6.82E − 11	6.82E − 11	6.82E − 11	6.81E − 11	6.65E − 11	5.72E − 11	3.22E − 11	7.37E − 15
Zr-95	1.09E − 11	1.09E − 11	1.09E − 11	1.09E − 11	1.08E − 11	1.01E − 11	7.87E − 12	2.10E − 13
Nb-97m	7.34E − 12	7.34E − 12	7.34E − 12	7.05E − 12	2.72E − 12	~0	~0	~0
Nb-97	6.96E − 12	6.96E − 12	6.96E − 12	6.94E − 12	2.78E − 12	~0	~0	~0
Nb-95	1.38E − 11	1.38E − 11	1.38E − 11	1.38E − 11	1.37E − 11	1.34E − 11	1.19E − 11	4.71E − 13
Co-60	8.67E − 13	8.67E − 13	8.67E − 13	8.67E − 13	8.67E − 13	8.65E − 13	8.58E − 13	7.60E − 13
others	2.20E − 12	2.20E − 12	2.19E − 12	1.87E − 12	6.46E − 13	6.07E − 14	4.68E − 14	1.25E − 15

4. Summary

The objective of this study was to calculate activities and the dose rates for the dosimetry foils at OLTIS induced by neutron irradiation in complex scenario of TT campaign. Subsequent activities and dose rates at shutdown were calculated by means of the FISPACT-2010 code using the irradiation scenario specified for JET. With the neutron flux densities and spectra provided by the preceding MCNP neutron transport calculation. After the end of irradiation, the activities and doses are calculated at the cooling time of 0 and 1 s, 1 h, 1 day, 1 week, 1 month,

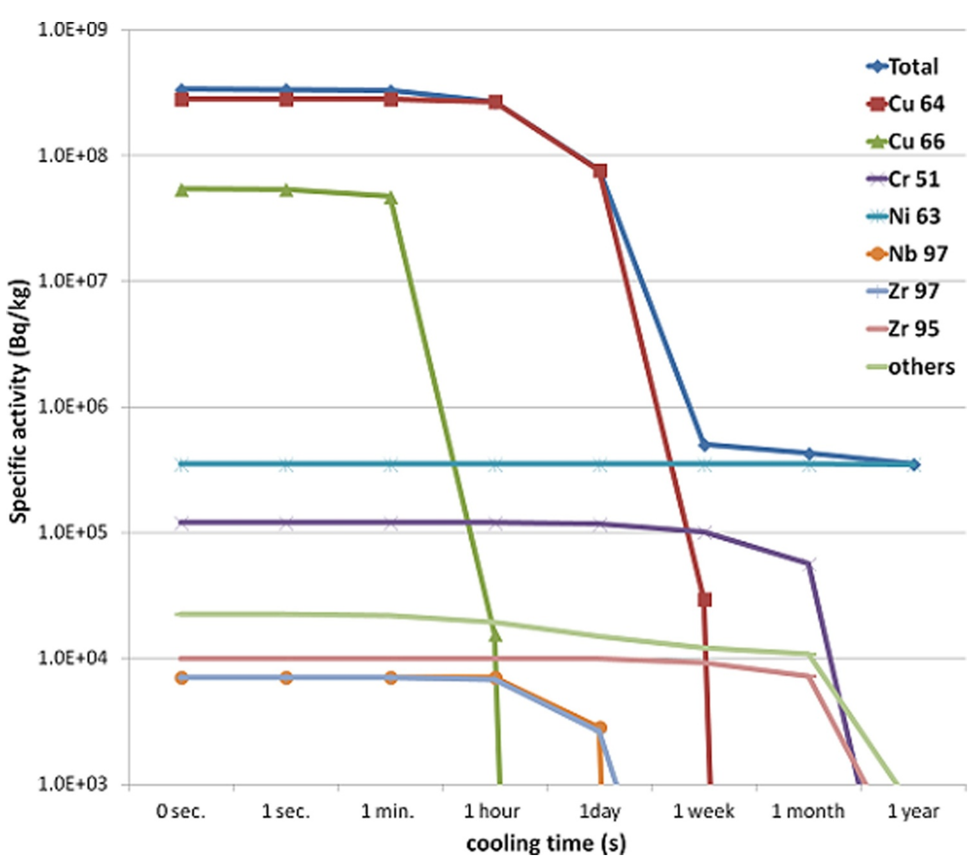

Fig. 7. Specific activity at OLTIS for CuCrZr.

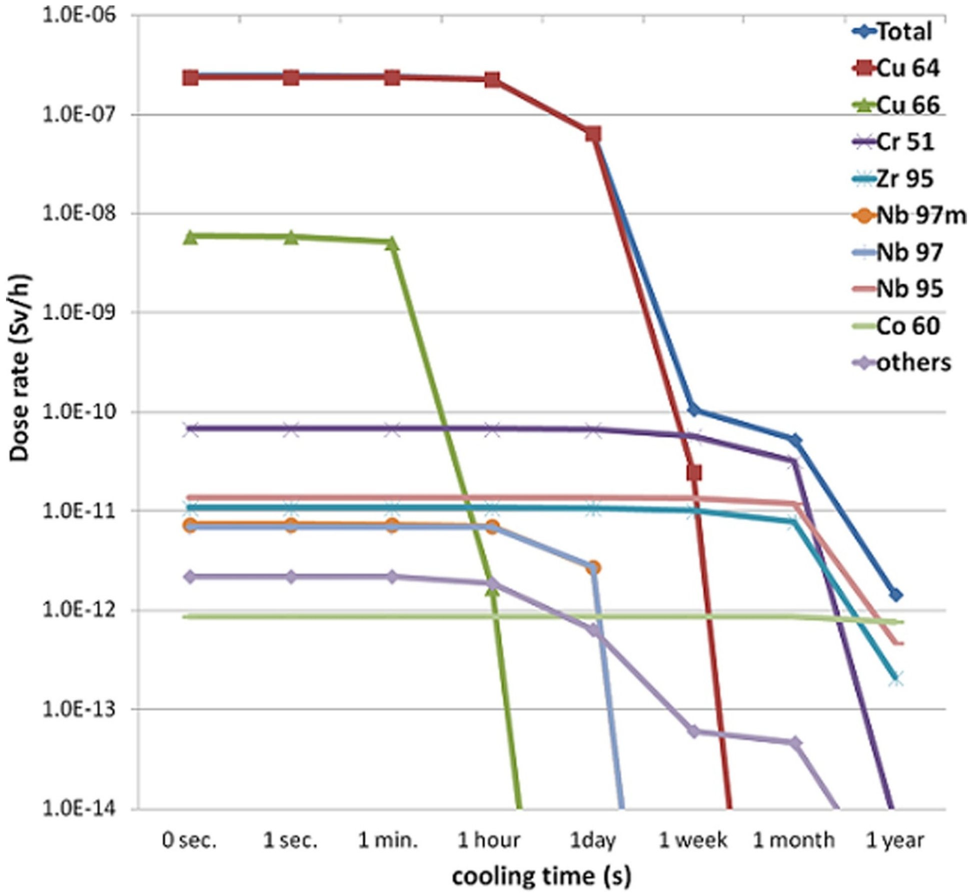

Fig. 8. Dose rate at 30 cm distance from the point source for CuCrZ.

1 year.

Investigation of the copper based materials (Al-Bronze and CuCrZr) shows that the total contact dose rate values range from 2.71×10^{-7} to 1.23×10^{-2} Sv/h throughout the investigated cool down periods. Dose rates values at 30 cm distance from the source range from $1.4\ 10^{-12}$ to $2.23\ 10^{-7}$ Sv/h with the highest value being found in Al-Bronze. Total specific activity for metal samples range from 3.52×10^5 to 3.37×10^8 Bq/kg. 1 year after the end of irradiation higher dose rate and activity values were also present in Al-bronze alloy compared to CuCrZr. In this case after 1 year these two materials could be Low-level waste.

The study of two copper based alloys identified the Cu-64 at the beginning of observation and Ni-63 at the end as the largest contributors to the total activity while Cu-64 at the beginning of cooling time and Co-58 and Co-60 at the end, were found to be the major contributors to the dose rate.

Declaration of Competing Interest

None.

Acknowledgments

This work has been carried out within the framework of the EUROfusion Consortium and has received funding from the Euratom research and training programme 2014–2018 and 2019–2020 under grant agreement No 633053. The views and opinions expressed herein do not necessarily reflect those of the European Commission.

References

[1] E. Joffrin, et al., Overview of the JET preparation for deuterium/tritium operation with the ITER like-wall, Nucl. Fusion (2019).
[2] E. Joffrin, et al., Overview of the JET preparation for Deuterium-Tritium Operation" IAEA 27th Fusion Energy Conference, Ahmedabad, India, 2018 October 22-27.
[3] E. Belonohy, et al., Technical rehearsal of tritium operation at JET, Fusion Eng. Des. 123 (2017) 196–200.
[4] L.W. Packer, P. Batistoni, et al., Status of ITER material activation experiments at JET, Fusion Eng. Des. 124 (2017) 1150–1155.
[5] G. Kalinin, V. Barabash, et al., Assessment and selection of materials for ITER in-vessel components, J. Nucl. Materials 283-287 (2000) 10–19.
[6] V. Barabash, et al., Materials challenges for ITER – current status and future activities, J. Nucl. Materials 367-370 (2007) 21–32.
[7] Cu-Cr-Zr - Chemical Composition (ITER_D_223247 v2.0).
[8] Aluminium bronze forgings specification for divertor cassettes(ITER_D_73yyhw v1.3).
[9] F. Brown, B. Kiedrowski, J. Bull, M. Gonzales, N. Gibson, Verification of MCNP5-1. 60, LA-UR-10-05611 (2010).
[10] R.A. Forrrest, The FISPACT-2007 User Manual, Culham Science Centre, 2007.
[11] L.W. Packer, J-Ch. Sublet: The European activation file: EAF-2010 decay data library, CCFE-R (10)02, March (2010).
[12] G. Stankunas, A. Tidikas, A. Cufar, Activation inventories after exposure to DD/DT neutrons in safety analysis of nuclear fusion installations, Radiat. Prot. Dosimetry 180 (2018) 125–128.
[13] Department of Energy and Climate Change, The Scottish government, welsh government and department of the environment Northern Ireland, UK strategy for the management of solid low level waste from the nuclear industry, (2016).